Telecommunications and Radio Engineering, 77(11):925-943 (2018)

ANTENNAS

DIFFRACTION ANTENNAS. SYNTHESIS OF RADIATING ELEMENTS

S.S. Sautbekov,[1] K.Yu. Sirenko,[2] Yu.K. Sirenko,[2,♦] & A.P. Yevdokymov[2]

[1]*Al-Farabi Kazakh National University, 71 al-Farabi Ave., Almaty 050040, Republic of Kazakhstan*

[2]*O.Ya. Usikov Institute for Radio Physics and Electronics, National Academy of Sciences of Ukraine,12 Academician Proskura St., Kharkiv 61085, Ukraine*

♦Address all correspondence to: Yu.K. Sirenko, E-mail: yks@ire.kharkov.ua

The synthesis of radiating elements of the diffraction antennas is reduced to providing a required amplitude and phase distribution of the field across the aperture. The field distribution is formed by the "dielectric waveguide-grating" system with satisfying a number of additional requirements associated, basically, with minimizing the amount of loss in the elements of the feeding section and optimizing the antenna radiation efficiency and accounting the factor of possible phase distortions. Rather difficult problems that are faced in this case are solved within the frame of an approach that effectively use the possibilities of both experimental and theoretical methods. Specific features of applying this approach to constructing linear diffraction gratings on the basis of ridged dielectric waveguides are considered in this paper

KEY WORDS: *linear diffraction radiation antenna, periodic grating, ridged dielectric waveguide, surface-to-spatial mode conversion, amplitude and phase field distribution across the radiating aperture*

1. INTRODUCTION

A flat density modulated electron beam flying at a constant rate over an infinite one-dimensionally periodic grating produces uniform plane electromagnetic waves in the surrounding space. The number, wavelength and propagation direction of the waves is determined by the rate and modulation period of the flow and also by the grating period. The field of the plane waves arising in the above described situation above or under the grating is generated by the proper filed of the charged particles flow. This way one can conceive the well-known Smith-Purcell effect on implementation of wave analogs of which the so-called diffraction antennas are constructed. The present study

0040-2508/18/$35.00

is focused on the problems of synthesis of radiating elements of such antennas. We call the wave analogs of the Smith-Purcell radiation phenomenon the effects of surface-to-spatial mode conversion as follows. A surface wave of an open guiding structure, whose field is in many aspects similar to the eigenfiled of a flow of charged particles, sweeping by its exponentially decaying part the grating surface, generates in the radiation zones of the periodic structure spatial waves capable of propagating infinitely far in the absence of attenuation here.

The diffraction effects (effects of diffraction radiation) were sequentially and thoroughly studied during the last two decades of the past century in the O.Ya. Usikov Institute for Radio Physics and Electronics of the National Academy of Sciences (IRE NASU), Kharkiv, Ukraine, in the department headed, at that time, by academician Victor P. Shestopalov. In this respect, rather useful has proven to be the experience accumulated there in the process of developing the so-called generators of diffraction radiation which represent stable, coherent sources of millimeter wave electromagnetic oscillations operating on the basis of the Smith-Purcell effect. Above all, this concerned theoretical representations about the processes of resonance scattering of plane waves by periodic structures soundness of which has rather convincingly been confirmed by practice. The Smith-Purcell effect was theoretically studied in the specified current approximation and within the frame of two-dimensional scalar models where an infinite one-dimensionally periodic grating was “placed” in the field of a non-uniform plane wave. However, even such approach in combination with well-prepared natural experiments has made it possible to effectively solve all the basic problems associated with creation of the unique in its characteristics source of electromagnetic waves.

The appropriate methodology has successfully been used by the team of Stanislav D. Andrenko (V.G. Belyayev, V.V. Kryzhanovskiy, A.P. Yevdokymov, S.A. Provalov, and Y.B. Sidorenko) and for construction of the first laboratory prototypes and experimental samples of the diffraction radiation antennas or, simply, diffraction antennas implementing a wave analog of the Smith-Purcell effect.

The design of antennas for radar and radiometric complexes capable of effectively solving specific practical problems and, in particular, problems of remote sensing of the Earth from aerospace carriers have required developing and implementing in the research practice new theoretical and experimental approaches and methods whose use allowed providing acceptable characteristics of the developed devices. The faced problems were basically associated with analysis and synthesis of open waveguides of various types, creation of effective their exciters, with providing a specified amplitude and phase field distribution across the radiator apertures, with the development and implementation of simple circuits of electromechanical beam scanning, and with sufficiently reliable electrodynamic modeling and analysis of both separate elements and units of the diffraction antennas and antennas of the kind on the whole.

A description of one of such approaches that allow effectively synthesizing radiating elements of the diffraction antennas makes the basic content of the paper.

2. SYNTHESIS OF RADIATORS WITH A SPECIFIED AMPLITUDE AND PHASE DISTRIBUTION OF THE FIELD ACROSS THE APERTURE

Consider a radiator whose basic elements are a ridged dielectric waveguide (RDW) and a reflecting lamellar grating (see Fig. 1, where $a_1 = 7.0$ mm, $b_1 = 7.0$ mm, $a_2 = 40$ mm, $b_2 = 2.4$ mm, $a_3 = 4.0$ mm, $b_3 = h$, $a_4 = 77$ mm, and $b_3 + b_4 = 5.5$ mm). A radiator like that, in particular, was used in the antenna for an 8-millimeter-range airfield control radar [1].

The dielectric waveguide made of fluoroplastic with $\varepsilon = 2.05$ supports propagation of the surface EH_{11} -mode the velocity factor of each is $\gamma(k) = \beta^{-1}(k) = \bar{\chi}(k)/k = 1.243$ for $\lambda = 2\pi/k = \lambda_{\text{work}} = 8.3$ mm, with λ_{work} being the working wavelength, $\beta(k)$ the relative phase velocity and $\bar{\chi}(k)$ the propagation constant of the surface wave. The E_y and E_z components are dominant in the electric field $\vec{E}$ of this wave. Being scattered by the grating, it generates an outgoing spatial wave with the horizontal polarization of the field. The $\vec{H}$ -vector of this wave is oriented practically perpendicular to the plane of symmetry of the structure $y0z$, that, with account of the spatial orientation usual for the linear antennas, we call the horizontal one.

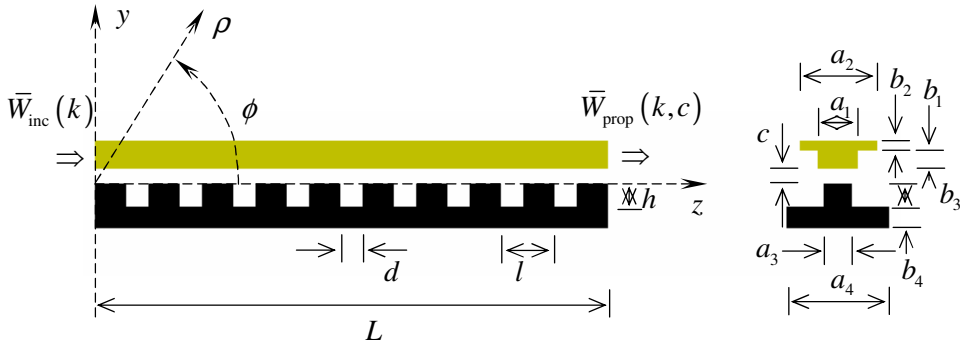

FIG. 1: Electrodynamic layout of the "ridged dielectric waveguide-grating" radiator

In order to construct an effectively operating antenna on the basis of the radiator under consideration, it is necessary to solve three key problems as follows [2,3].

The first problem consists in determining the length l of the grating period and its structure (parameters d and h) proceeding from the requirements as follows. First, the slow surface wave with the propagation constant $\bar{\chi}(k) = \Phi_1(k)$ should generate in the reflection zone of the infinite periodic structure the only one (zero-order) propagating spatial harmonic and this harmonic should leave the grating within the angular sector $90° < \phi \le 130°$ $(\varphi_0(k) = \alpha_0(k) + 90° \in (90°, 130°])$. Second, the efficiency

of the surface-to-spatial wave conversion (this characteristic for planar infinite gratings is determined by the value $W_{01}(k)$) should be sufficiently high, and phase distortions (variations in the $\overline{\chi}(k)$ magnitude due to the waveguide-grating field coupling) should be minimum. Here (see references [2,4,5]) $\Phi_n(k)$ is the longitudinal (along the z-axis) propagation constant of the n-th spatial harmonic of the periodic structure, $\alpha_n(k) = -\sin^{-1}[\Phi_n(k)/k]$ is the angle at which such propagating harmonic leaves the grating in its reflection zone (counted within the $y0z$-plane anticlockwise from the y-axis), and $W_{np}(k)$ is the portion of the scattered power that is fed-out into n-th propagating harmonic given the grating is excited by the p-th uniform (propagating without decay) or non-uniform (damped) plane wave.

The second problem is to achieve a necessary field distribution across the radiator aperture through selecting (by means of bending the RDW) the proper separation c between the waveguide and grating throughout its length $0 \le z \le L$. Each local value of the impact parameter $c = c(z)$ on this interval of changing the z coordinate is correspondent to its own value of the radiated power and hence, its own value of the filed strength within the plane $y = const > c + b_1 + b_2$ on a segment of the straight line $0 \le z \le L$, $x = 0$, for example. Solution of this problem clears the way to constructing an antenna with a specified side-lobe level (SLL) of the directional pattern within the $y0z$-plane and with a required radiation efficiency [2,6].

The third problem consists in determining and minimizing the level of phase distortions on the radiator aperture, i.e., the value $\Delta\psi(z)$ of deviation of the field phase $\psi(z)$ from the straight line connecting the points $\psi(0)$ and $\psi(L)$ corresponding to the beginning $(z = 0)$ and end $(z = L)$ of the interaction region.

The result of experimentally solving the first problem is $l = 6.2$ mm, $d = 2.0$ mm, and $h = 1.5$ mm (see Fig. 1). A prototype of the radiator with a grating of length $L_{\text{prot}} = 250$ mm was used to measure the key characteristics of the "surface wave line-grating" system, namely, $\overline{W}_{\text{inc}}(k)/\overline{W}_{\text{prop}}(k,c)$ (see Fig. 2(a), where $\overline{W}_{\text{inc}}(k)$ and $\overline{W}_{\text{prop}}(k,c)$ are, respectively, the energy fed into the system and that transmitted at its output) and $\gamma(k,c)$ (see Fig. 2(b)) for various values of the impact parameter c. The $\gamma(k,c)$ dependences were measured with a 8-mm wavelength phase meter with a Doppler frequency shifter [7]. The value $\gamma(k)$ for various magnitudes of c was determined from the field phase incursion over the distance $0 \le z \le L_{\text{prot}}$, i.e., throughout the length of the waveguide – grating interaction region. The gagging equipment provided the measurement accuracy 0.2°. The input and output of the radiator prototype were both well-matched with the leading sections of the phase meter. Based on the measurement results, among several the most suitable gratings (a detailed analysis of the electrodynamic characteristics of periodic structures of the kind has been performed in [2,8-11]) that was selected which satisfied the above formulated

requirements in the best way. It can be expected that for the fixed with this values $l = 6.2$ mm and $\lambda = \lambda_{\text{work}} = 8.3$ mm the direction of departure of the radiated wave within the $y0z$-plane will be determined by the angle

$$\begin{aligned}\varphi_0(k) &= 90° - \sin^{-1}(\Phi_0 / k) = 90° - \sin^{-1}\left[\bar{\chi}(k) / k - 2\pi / (lk)\right] = \\ &= 90° - \sin^{-1}\left[\gamma(k) - \lambda / l\right] = 90° - \sin^{-1}(1.243 - 1.339) = 95.49°.\end{aligned} \tag{1}$$

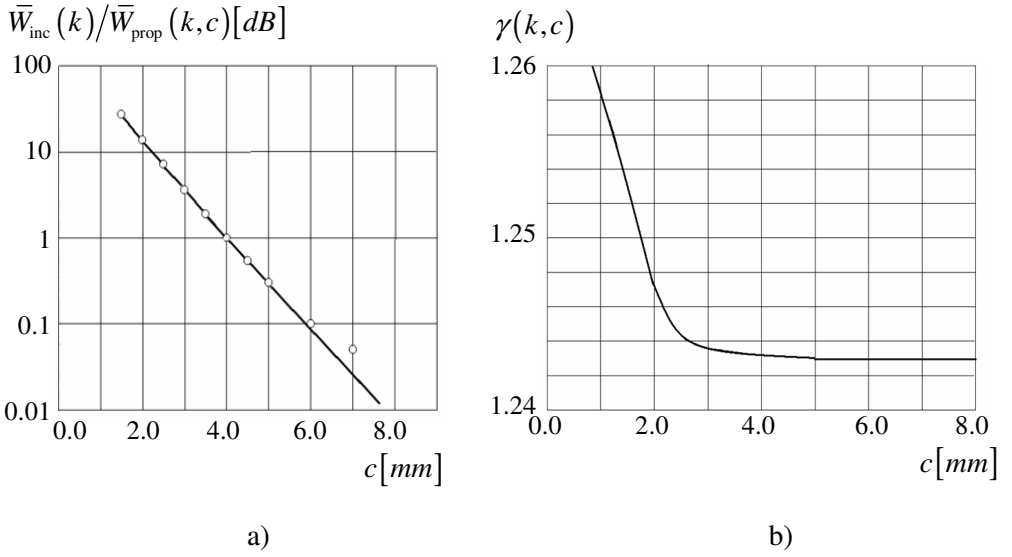

a) b)

FIG. 2: Power characteristics (a) and velocity factor of the system "ridged dielectric waveguide-grating" measured using a mock-up of the radiator 250 mm in length (b)

The field strength of a planar dielectric waveguide decreases in the outer space with distance $r > 0$ from its surface according to the law $\exp[-\alpha(k)r]$, where $\alpha(k) = \text{Im}\sqrt{k^2 - \bar{\chi}^2(k)}$ [2]. An RDW differs from the planar waveguide with the same velocity factor by that its field decreases more sharply with the distance from its surface faced to the grating following a law that can approximately be described by the formula $\exp[-\alpha(k)r]\sqrt{r_0 / (r_0 + r)}$, where r_0 is the distance from the point of maximum power flux density within the transverse section of the RDW to the plane $z = c$ (see Fig. 1).

The characteristic of power take-off corresponding to this law for the parameters $\gamma(k) = 1.243$, $k = k_{\text{work}} = 2\pi / \lambda_{\text{work}}$ and $r_0 = 3.0$ mm is shown in Fig. 2(a) by the solid line. The dependence has been constructed using data calculated from the

experimentally determined value $\overline{W}_{\text{inc}}(k)/\overline{W}_{\text{prop}}(k,c)$ with $c=1.5$ mm and is in good agreement with the measurement results (circles) for greater (up to $c=5.0$ mm) distances between the RDW and grating. The calculated data obtained in this way are necessary to accurately determine the $c(z)$-profile along the entire interaction region when it happens to register in some points of the interval $0\le z\le L$ attenuations under 10^{-4} dB with the values $c\approx 12.0$ mm ($c\approx 1.45\lambda_{\text{work}}$). The matter is that the range of sufficiently accurate measurements of the attenuation makes $1.0\div 30.0$ dB, and the increased errors of measuring the power take-off in the range of its small values is the reason for the discrepancy between the experimental and calculated data in Fig. 2(a) for the levels below 0.1 dB.

At the next stage, when solving the second problem, we fixed the total length of the radiator to be $L=8L_{\text{prot}}=2000$ mm, that allowed obtaining a rather narrow-beam directional pattern within the $y0z$-plane, and used the dependence $\overline{W}_{\text{inc}}(k)/\overline{W}_{\text{prop}}(k,c)$ that had already been obtained for the radiator prototype of length 250 mm (see Fig. 2(a)). Making use of the specified amplitude distribution of the field across the antenna aperture (this characteristic is determined, in particular, by the function $\overline{W}_{\text{rad}}^{\text{norm}}(k,z)=\overline{W}_{\text{rad}}(k,z)\Big/\max\limits_{0\le z\le L}\left[\overline{W}_{\text{rad}}(k,z)\right]$ of the normalized distribution of the radiated wave power, antenna efficiency and amount of linear loss in the surface wave line, the necessary level of the power take-off by each of the eight short radiating elements was calculated. Then, using the $\overline{W}_{\text{inc}}(k)/\overline{W}_{\text{prop}}(k,c)$-dependence, the value of c was determined for each of these elements to construct, finally, the $c(z)$-dependence for the entire length of the interaction region. Under the condition of providing a sufficiently high measurement accuracy, this approach demonstrates good agreement between the calculated and expected data.

In the course of stating and solving the second problem, it is necessary to take into account a number of general limitations imposed on the shape

$$f(z)=\varsigma+(1-\varsigma)g\left(\frac{2z-L}{L}\right);\quad 0\le\varsigma\le 1,\quad \left|p=\frac{2z-L}{L}\right|\le 1,\quad 0\le g(p),\quad \max_{|p|\le 1} g(p)=1$$

of the specified amplitude distribution of the field along the radiator aperture $0\le z\le L$. Specifically, the respective curve should be sufficiently smooth and, being represented on a linear scale, should not contain zeroth values of the amplitude, including magnitudes at the edges of the interaction region. For this reason, such popular distributions like cosine, $g(p)=\cos(p\pi/2)$ (see [6] and Table 4.1), and squared-cosine, $g(p)=\cos^2(p\pi/2)$, can be implemented only with a "pedestal" ς no less than 0.01 in height. Note in this connection that the pedestal $\varsigma=0.1$ in the case of the squared-cosine distribution provides the value of the first lidelobes at the level -42.64 dB.

Now, let us briefly describe the sequence of steps whose realization makes it possible to provide an amplitude distribution of the field on the aperture close to the specified one.

– The radiator efficiency $\eta \le 1$ (the $\overline{W}_{\text{rad}}$ -to- $\overline{W}_{\text{inc}}$ value ratio), expected amplitude distribution $f(z)$, the rate of decreasing the field strength at the aperture edges, and linear loss in the surface wave line are specified.

– The aperture $0 \le z \le L$ is divided into N equal in length segments A_j, with $j = 1, 2, \ldots, N$, whose midpoints correspond to the coordinates $z_j = \frac{L}{N}(j - 0.5)$.

– Potentiation of the rate of decreasing the field power (specified in dB) at the aperture edge in the point z_N makes it possible to determine the relative amplitude $f(z_N)$, relative "power" $f^2(z_j)$ at every of the points z_j and normalization factor $\sigma = \sum_{j=1}^{N} f^2(z_j)$.

– The figure of the radiation efficiency η is used to determine the normalized power that should be radiated by each of the segments A_j of the radiator aperture, $w_j^{\text{rad}} = \eta \cdot f^2(z_j) / \sigma$.

– The input power $\overline{W}_{\text{inc}}$ is equated to unity and a set of parameters is sequentially determined for each of the aperture segments A_j, including the normalized input power $w_j^{\text{inc}} = w_j^{\text{prop}}$, with $w_1^{\text{inc}} = 1$; the normalized transmitted power $w_j^{\text{prop}} = w_j^{\text{inc}} - w_j^{\text{rad}} - w_j^{\text{abs}}$ ($w_j^{\text{abs}} = w_j$ is the normalized absorbed power whose value is determined by the specified level of linear loss and is taken into account in calculating the efficiency, $\eta = 1 - Nw^{\text{abs}} - w_{2N}^{\text{prop}}$) and the level of the power take-off, $10\lg(w_j^{\text{inc}} / w_j^{\text{prop}}) = w_j^{\text{inc}} / w_j^{\text{prop}}$ [dB].

– The measurement results like those presented in Fig. 2(a) are recalculated to the length of the segment A_j and used to determine the values $c(z_j)$ from the values $w_j^{\text{inc}} / w_j^{\text{prop}}$ [dB].

Seemingly, increasing N we improve the accuracy of solving the posed problem. This is so in the theory. However, in practice the value N is determined by the admissible number of points at which the position of the dielectric waveguide is fixed, flexibility of the material which it is made of and so on.

The already obtained dependences $c(z)$ for $0 \le z \le L$ and $\gamma(k, c)$ make it possible to solve the third problem, i.e., to calculate the level of phase distortions in the radiator aperture associated, generally, with a rather noticeable dependence of the velocity factor $\gamma(k)$ on the value of the gap c (see Fig. 2(b)).

The moderating coefficient $\gamma(k,c)$ starts to sharply vary with $c < 2.5$ mm. For this reason, this value is preselected as the maximum permissible one. The field phase $\psi(z)$ on the radiating aperture at the point z corresponding to a certain specific period of the grating is determined as a sum of phase incursions over all the periods preceding that under investigation. And these incursions are easy to be calculated using the local values of $\gamma(k,c)$ corresponding to each period and the value of the impact parameter c associated with this period. It seems difficult to estimate the difference $\Delta\gamma(k,c) = \gamma(k,c) - \gamma(k,\infty)$ for $c > 3.0$ mm on the scale used in Fig. 2(b). For this reason, we present some numerical values. These are $\Delta\gamma(k,c) = 6.5 \cdot 10^{-4}$ for $c = 3.0$ mm, $\Delta\gamma(k,c) = 2.3 \cdot 10^{-4}$ for $c = 4.0$ mm, and $\Delta\gamma(k,c) = 4.6 \cdot 10^{-5}$ for $c = 5.0$ mm. For the radiators with apertures greater than 100 wavelengths in size, even so small deviations require to take into account their influence on the directional pattern.

Now, let us see how the above described approach to solving the synthesis problem is implemented by way of example of constructing a radiator with beamwidth of the directional pattern within the horizontal plane $y0z$ equal to approximately $0.3°$, $\eta = 75\%$ and SSL no greater than -20 dB. Obtaining such characteristics can provide a cosine amplitude distribution with the pedestal $\varsigma = 0.03$ (voltage drop at the aperture edges is -30 dB). The solid line in Fig. 3(a) shows the $c(z)$-profile calculated for this distribution with account of the linear loss in the dielectric waveguide at the level 0.85 dB/m. The extreme (minimum and maximum) magnitudes of the value c within the interaction region are equal to 3.15 mm and 9.7 mm. The dashed line in Fig. 3(a) corresponds to the $c(z)$-profile in the constructed radiator presented in Fig. 4. The discordance between the calculated and implemented $c(z)$-dependences is associated with the fact that the necessary bending of the RDW was provided by its fixing at only eight inner points of the interval $0 \le z \le L$ starting from the point $z = 125$ mm and then through each 250 mm. For the same reason, the value of the field drop at the aperture edges in the constructed radiator decreased from the expected -30 dB to -20 dB (see Fig. 3(b)).

The experimental and expected (specified) values of the function $W_{\text{rad}}^{\text{norm}}(k,z)$ reflecting the amplitude distribution of the field across the radiator aperture are in fairly good agreement. The total loss of the "RDW-grating" structure make 1.25 dB. This value includes the loss in the material of the guiding line and loss in the matched load at the end of this line.

Figure 5(a) presents the function $\Delta\psi(z)$, that determines the level of phase distortions on the radiator aperture, calculated from the dependence $\gamma(k,c)$ for the real profile $c(z)$. The calculated directional patterns of the radiator $D(\phi,k)$ for the cosine amplitude distribution on a pedestal without phase distortions and for real amplitude and phase distribution (see Figs. 3(b) and 5(a)) are shown in Fig. 5(b) by the solid and

dashed lines, respectively. The total impact of amplitude and phase distortions is insignificant. Specifically, the directional pattern maximum is slightly shifted toward the normal to the aperture, a minor asymmetry is observed in the sidelobes whose level demonstrates even a decrease. The key conclusion consists in that the eight points of fixing an RDW is quite enough to obtain an amplitude distribution of the field across the aperture of length 2000 mm which is close to the specified one.

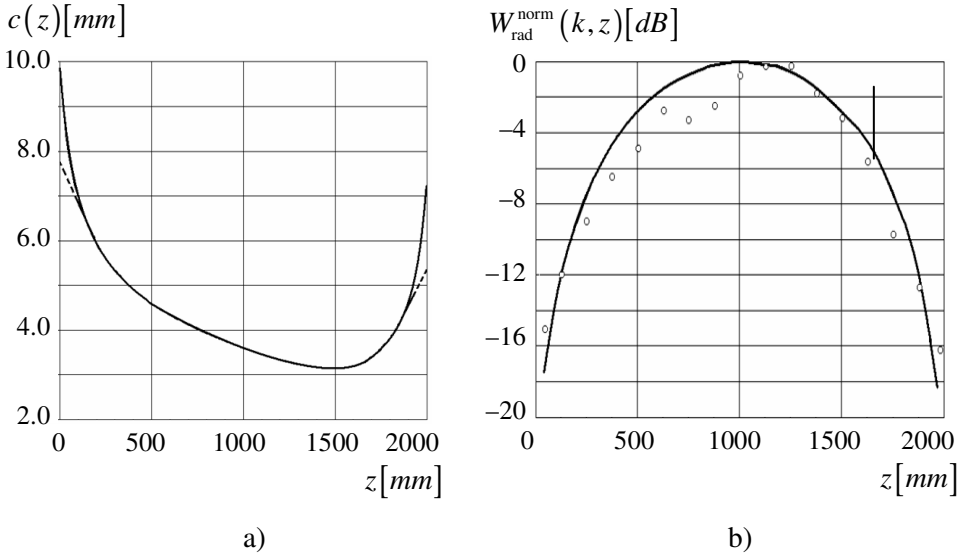

FIG. 3: Values of the impact parameter $c(z)$ (a) and expected (solid line) and measured (circles) distributions of the radiated wave power across the antenna aperture $0 \le z \le L$ (b)

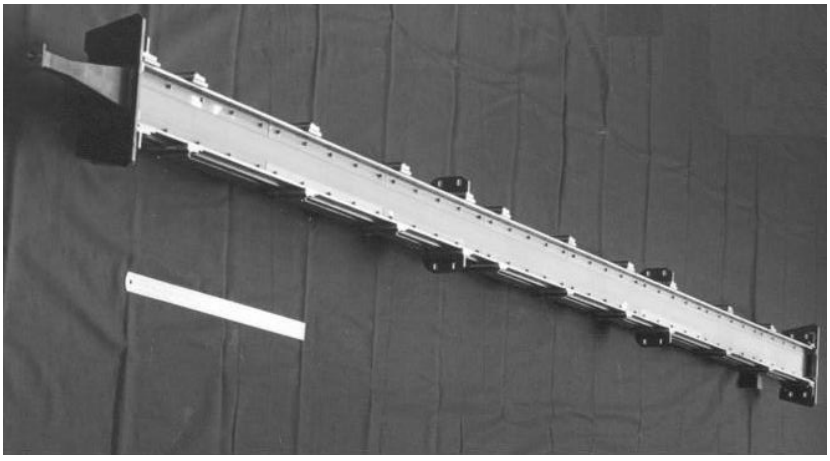

FIG. 4: Experimental prototype of the radiator

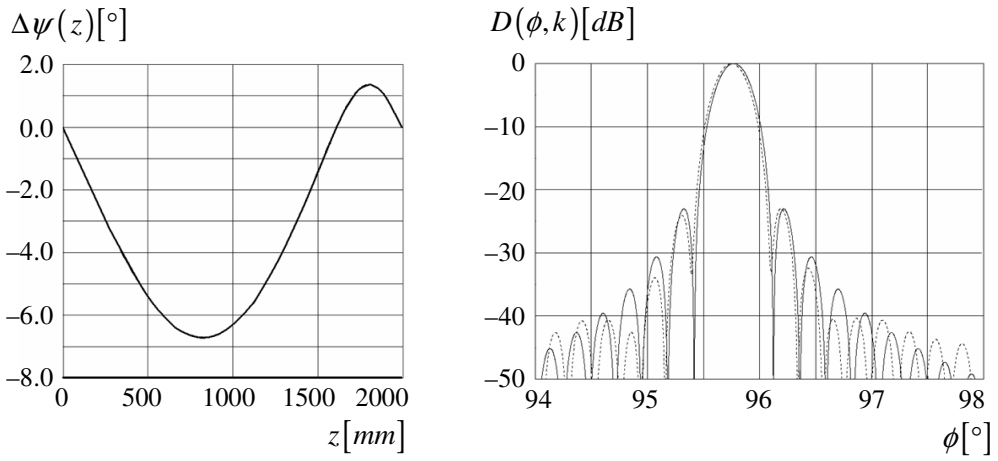

FIG. 5: The level of phase distortions on the radiator aperture $0 \le z \le L$ (a) and calculated directional patterns of the antenna within the horizontal plane illustrating the impact of phase and amplitude distortions on the aperture (b)

The real directional pattern of the radiator within the $y0z$-plane is shown in Fig. 6. Its beamwidth is $\phi_{0.5} = 0.27^\circ$ (or $\varphi_{-3.0\text{dB}} = 0.27^\circ$), the sidelobe level is -21.7 dB. Comparison of the calculated (see Fig. 5(b)) and experimentally obtained SLLs demonstrates that there are some additional unaccounted sources of amplitude and phase distortions in the produced radiator. However, the observed excess of the real SLL over the calculated one has proven to be insignificant (less than 1.2 dB) and quite acceptable. Probably, this is also because the influence of such sources like errors in manufacturing of the periodic structure and nonflatness of its surface had been minimized in the design under measurements. Generally, all these sufficiently good results have been provided to a considerable extent by the optimum selection of the dielectric waveguide dimensions and sizes that unambiguously determine the grating geometry.

Note that the experimental data presented above have been obtained at the frequencies k_{work} (f_{work}) corresponding to the wavelength $\lambda = \lambda_{\text{work}} = 8.3$ mm. The radiator (see Fig. 4) is equipped with a horn transition from a rectangular waveguide with transverse section $a \times b = 7.2 \times 3.4$ mm^2 the total loss of which are equal to 0.2 dB, with 0.1 dB of which being the radiation loss. The standing wave ratio (SWR) of the radiator does not exceed 1.15 over the frequency range $f = 34 \div 38$ GHz ($7.89\text{ mm} \le \lambda \le 8.82\text{ mm}$).

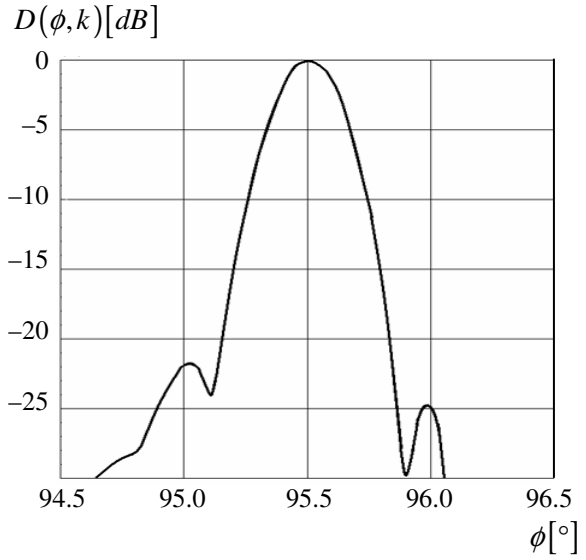

FIG. 6: Measured directional pattern of the radiator within the horizontal plane

The width of the directional pattern of the radiator within the $x0y$ (the vertical plane) is 42.5°. With increasing the grating width a_3 to the value about $2f_{\text{work}}$ and keeping the other parameters unchanged, the directional pattern in the vertical plane narrows to 20°. The constructed radiator with such parameters can be regarded as an independent device that can be used as an antenna of ship radars of side-looking radars. The device has the same limitations to the pulsed power as the standard units on the basis of a hollow metal waveguide. The admissible level of the mean power makes 200 W.

3. MAINTENANCE OF THE RADIATOR OPERABILITY IN THE CASE OF VARIATION OF THE LEVEL OF COUPLING BETWEEN THE GRATING AND SURFACE WAVE LINE

Listed in Table 1 are values of the function $c(z)$, realization of which in the radiator (see Fig. 1) with the parameters $l = 6.5$ mm, $d = 2.0$ mm, $h = 1.6$ mm, $L = 1830$ mm, $a_1 = 8.0$ mm, $b_1 = 3.5$ mm, $a_2 = 40$ mm, $b_2 = 2.7$ mm, $a_3 = 12.0$ mm, $b_3 = h$, $a_4 = 28$ mm, and $b_4 = 6.4$ mm, makes it possible to obtain for $\lambda = \lambda_{\text{work}} = 8.8$ mm a field distribution across the aperture close to the squared-cosine one with a drop at the edges up to -14 dB (see the first raw in Table 2).

TABLE 1: Calculated values of the impact parameter

$z[mm]$	10	110	310	510	710	910
$c(z)[mm]$	6.49	6.25	5.22	4.29	3.63	3.17
$z[mm]$	1110	1310	1510	1710	1810	
$c(z)[mm]$	2.88	2.80	3.11	3.79	3.95	

TABLE 2: On estimating the influence of uniform deviations in the values of the function $c(z)$

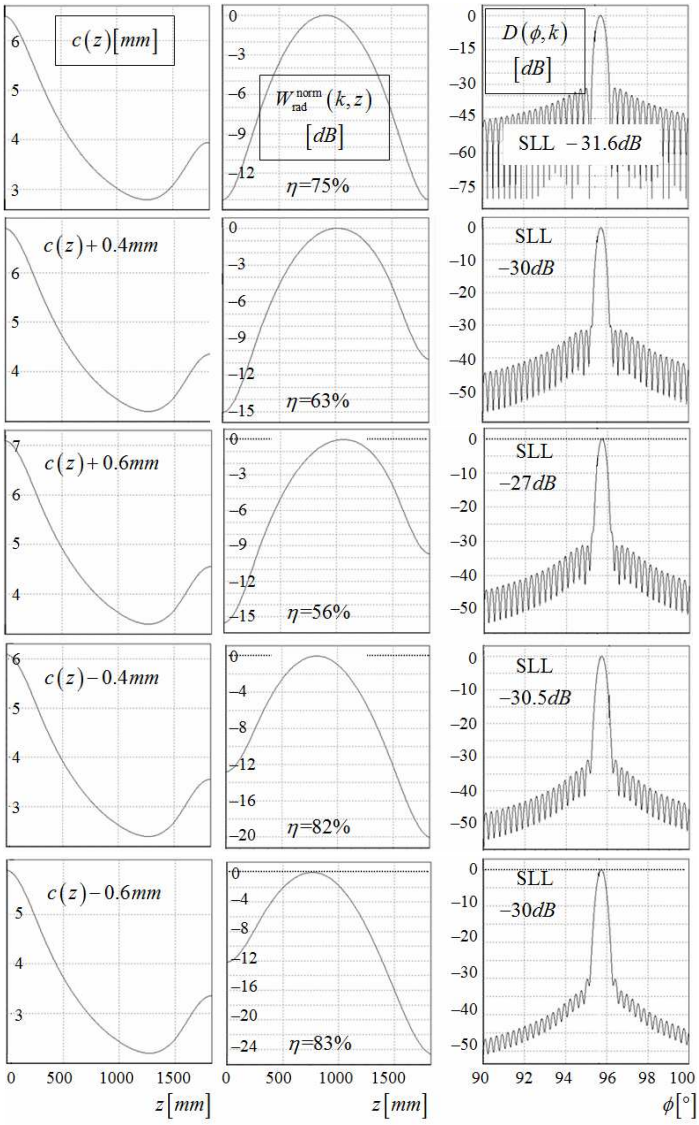

The power characteristics used for calculating the $c(z)$-profile have been taken from a radiator prototype of the length $L_{\text{prot}} = 201.5$ mm.

Listed in Table 2 are the calculation data that allow estimating the degree of influence of uniform (throughout the length of the interaction region) deviations in the values of the calculated function $c(z)$ (see the first raw). The first column in Table 2 (raw two to raw five) contains the new profiles of the impact parameter. The second and third columns present the field power distributions, radiator efficiency η and directional patterns that correspond to these profiles The main lobe beamwidth $\phi_{0.5}(k)$ in all the cases is equal to 0.325°. In the course of calculating the directional patterns phase distortions were disregarded. The considered value of the linear loss makes 1.0 dB/m.

Increasing the antenna efficiency is associated with the necessity to use the small impact parameters, however this leads to increasing the phase distortions. For this reason, selection of the field drop at the output from the interaction region to be at the level -14 dB ($\eta = 75\%$) seems to be optimum with respect to both the phase distortions and possible thermal expansion (contraction) of the radiator components, and metrics since it is quite difficult to reliably measure the field drop rate at the level -20 dB and lower.

Generally, the data listed in Table 2 indicate that a considerable uniform increase or decrease of the impact parameter value, associated, for example, with changes in the ambient temperature, do not result in disfunction of the radiator and a diffraction antenna on its basis. In the course of manufacturing such an antenna, quite large deviations of the $c(z)$ dependence from the initial, specified one are permissible on the whole.

Now, let us consider how deviation in the values of the primary function $c(z)$, that correspond to small intervals of changes in the z-coordinate, influence the radiator characteristics (see Table 3). Deviations of the kind can arise if in the course of the radiator mounting the $c(z)$ dependence is realized with the use of separate fixing points (see Table 1).

The first and second rows of Table 3 present results for the cases where the calculated value of $c(z)$ was increased by 0.2 mm and 0.4 mm, respectively, at one point of the aperture with the coordinate $z = 1100$ mm. Listed in the third and fourth rows are results obtained for the cases where the calculated value $c(z)$ at the same point was decreased in the same way. As expected, the radiator efficiency decreases in the first case and increases in the first one when the field coupling between the waveguide and grating at a small part of the interaction region though insignificantly but increases. Essential distortions of the amplitude distribution of the field across the aperture and considerable increase of the SLL are observed in all the cases considered. The presented data point out the inadmissibility of deviations of the $c(z)$-dependence at separate point to be greater than 0.1 mm. However, as was shown before, smooth and uniform changes of the impact parameter by an even much greater value lead to just insignificant changes in the radiator characteristics.

TABLE 3: On estimating the influence of local deviations in the values of the function $c(z)$

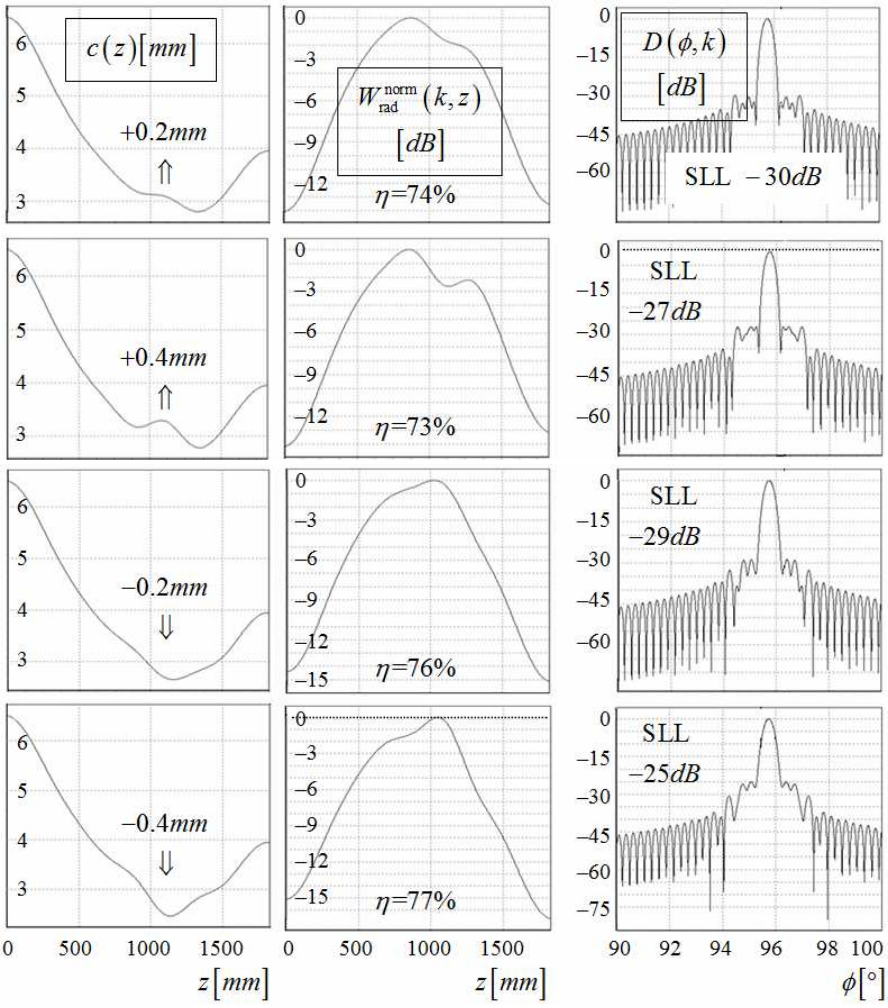

In conclusion we would like to note that the experimentally measured directional pattern within the $y0z$ for the initial parameters listed in Table 1 had the width coinciding with the calculated one, with the sidelobe level being no higher than -27 dB.

4. PRINTED GRATING IN THE DIFFRACTION ANTENNA RADIATOR

Replacement of the lamellar grating in the antenna radiator shown in Fig. 1 by a printed grating (see Fig. 7) would allow an increasing essentially the attractiveness of

the designs under discussion by a number of important factors. The results of references [9-12] allow stating that this replacement is quite feasible. There are needed only materials of sufficiently high quality for manufacturing the gratings and experimental verification of the operability of a radiator consisting of a ridged waveguide and a printed periodic structure coupled with the latter through the field. The second of these conditions we partially fulfill by representing in this Section experimental results that point to the conclusion that the difference between the power characteristics of lamellar and printed gratings are not fundamental and does not put obstacles in the way of using the latter in the capacity of one of the basic elements of the diffraction radiation antennas.

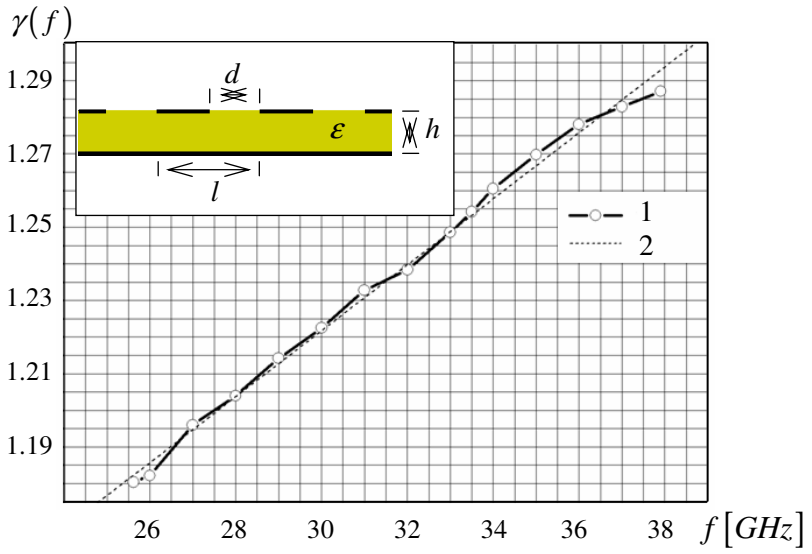

FIG. 7: Geometry of the printed grating and slowing factor $\gamma(f)$ of the exciting it the EH_{11}-mode of the ridged waveguide within the frequency. Curve 1 corresponds to the experiment while curve 2 represents its linear approximation.

In the experiments, we used a radiator prototype of length $L_{\text{prot}} = 140\,\text{mm}$ with a ridged waveguide whose characteristics we discussed at the final part of paper [13]. The case of horizontal polarization of the radiated field was considered, with the surface EH_{11}-mode being excited in the waveguide. Its experimentally determined velocity factor is shown in Fig. 4 (see also Fig. 11 in paper [13]). Four changeable strip gratings differing by the slot width alone d. To be specific, these were $d = 1.5\,\text{mm}$, $d = 2.5\,\text{mm}$, $d = 3.5\,\text{mm}$, and $d = 4.5\,\text{mm}$. The gratings were made of a sheet fluoroplastic ($\varepsilon \approx 2.05$) coated from both sides by copper foil. The height of the gratings was $h = 1.6\,\text{mm}$ and the length of the period was equal to $l = 6.5\,\text{mm}$.

The frequency range under analysis was $f = 27 \div 36$ GHz ($\lambda = 8.33 \div 11.1$ mm). The function $\gamma(f)$ within this range shows a monotonic increase from the value $\gamma \approx 1.195$ for $f = 27$ GHz to the value $\gamma \approx 1.275$ for $f = 36$ GHz. Accordingly, the angle of radiation ϕ_0 given by Eq. 1 varies from the value $\phi_0 = 120.8°$ for $f = 27$ GHz to the value $\phi_0 = 90.4°$ for $f = 36$ GHz.

The experimentally determined characteristics of the radiator (see, for example, Fig. 8) have shown that for the acceptable values of c ($c \geq 2.5$ mm; see Fig. 2(b)) and gratings with slot widths 2.5 mm, 3.5 mm, and 4.5 mm the factor $\overline{W}_{\text{inc}}(f)/\overline{W}_{\text{prop}}(f,c)$ of power take-off in the "RDW-printed grating" structure does not exceed 2.0 dB throughout the frequency range under analysis. This is plainly insufficient to construct an effectively operating diffraction radiation antenna of the standard length. The same can be pointed out about the grating with the slot width $d = 1.5$ mm if consider the frequencies $f > 31$ GHz.

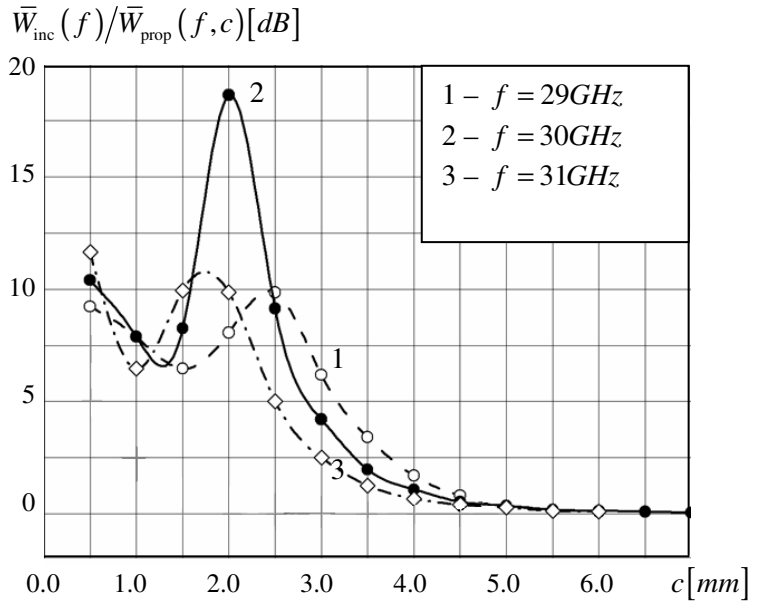

FIG. 8: Power characteristics of the system "ridged dielectric waveguide-printed grating" recalculated for the length of the radiator prototype equal to 130 mm and d = 1.5 mm

What remains are the range $f = 27 \div 31$ GHz and the grating with the slot width $d = 1.5$ mm. These are the parameters for which discussion of the possibility of creation of a linear "RDW-printed grating" radiator makes sense (see Fig. 8). Of course, this is within the frame of the limitations accepted here ($\varepsilon \approx 2.05$, $h = 1.6$ mm, and $l = 6.5$ mm).

We would like to notice one important difference in the behavior of $\overline{W}_{\text{inc}}(f)/\overline{W}_{\text{prop}}(f,c)$ for the lamellar (see Fig. 2(a)) and printed (Fig. 8) grating. The power take-off in the "RDW-printed grating" structure is associated not only with its transmission into free space, but also with energy transfer into the eigenmode of the open guiding line the role of which can be played by the grating under consideration on certain conditions [11]. These regimes of energy transfer are correspondent to vicinities of the local maxima in the dependences shown in Fig. 8. Obviously, it is necessary to avoid occurrence of the regimes like these in the synthesized radiators as they can decrease essentially the antenna efficiency.

Considering the stated above, let us briefly dwell on calculation of a radiator with the expected sidelobe level less than -30 dB. The input data will be the selected working frequency $f_{\text{work}} = 29$ GHz ($\lambda_{\text{work}} = 10.34$ mm), slowing factor $\gamma(f_{\text{work}}) \approx 1.215$ (see Fig. 7); radiator length $L = 2000$ mm, the characteristic shown by curve 1 in Fig. 8, linear loss in the RDW equal to 0.85 dB/m, and the radiator efficiency $\eta = 80\%$.

The specified side lobe level can be provided by the squared-cosine distribution of the field strength across the radiator aperture with falling at the edges to -14 dB [6]. This distribution and the profile $c(z)$ providing its realization are shown in Fig. 9. Presented in Fig. 10 is the directional pattern of the radiator calculated with neglect of phase distortions that are insignificant for such impact parameters. Its main lobe is pointed at the angle $\overline{\phi} = \phi_0 \approx 112.1°$ such as would be expected proceeding from the formula Eq. (1). The beamwidth is $\varphi_{0.5} = 0.375°$, the side lobe level makes -32 dB.

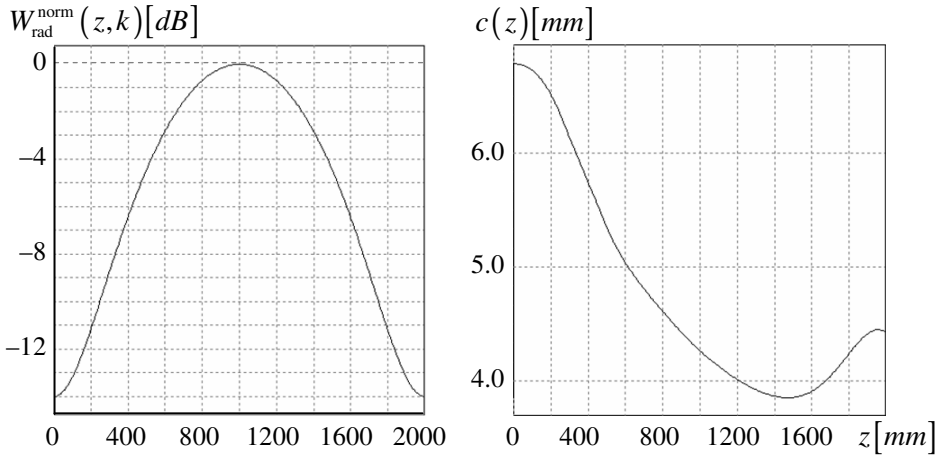

FIG. 9: The expected power distribution $W_{\text{rad}}^{\text{norm}}(z,k)$ across the radiator aperture (a) and values of the impact parameter $c(z)$ that can be provided by such distribution

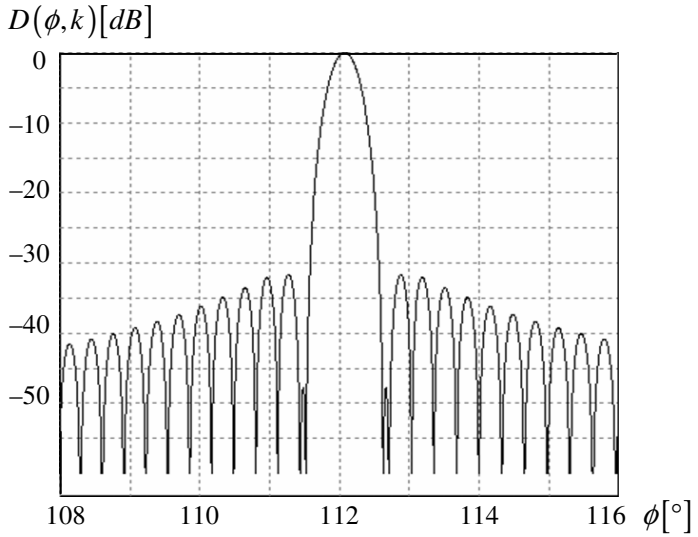

FIG. 10: Directional pattern of the radiator within the horizontal plane

It can be stated with sufficient confidence that the presented characteristics of the radiator, that have been obtained in the frame of standard theoretical considerations based on the results of experiments with its shortened prototype, will basically be duplicated in a real device should it be made with sufficient accuracy. And this means that the use of printed gratings in the radiators of diffraction antennas is possible though requires, of course, additional justification in the frame of problem-oriented theoretical and experimental investigations.

5. CONCLUSIONS

The electrodynamic scheme within which diffraction radiation antennas function is easy to implement in both computational models and laboratory prototypes of the respective devices that allow investigating practically interesting features in the physics of the occurring wave processes and conducting search of any kinds of the possibilities for their optimization and the most efficient application of the obtained theoretical and experimental results [2,3,14-18]. However, much more complex problems arise in the course of constructing antennas intended for operation in the modern radar and radiometric facilities of various application. These are the problems of synthesis with rather rigid constraints to the range of changes of the variable parameters and specific requirements to the electrodynamic characteristics of the device. For solving problems of the kind, special-purpose, problem-oriented approaches are developed with one of which being briefly described in the given paper.

REFERENCES

1. Yevdokymov, A. and Kryzhanovskiy, V., (2008) Antenna for an 8-millimeter wave airfield control radar, *Elektromagnitnye Volny and Elektronnye Sistemy*, **13**(6), pp. 46-53, (in Russian).
2. Sautbekov, S., Sirenko, K., Sirenko, Y., and Yevdokymov, A., (2015) Diffraction radiation phenomena: Physical analysis and applications, *IEEE Antennas and Propagation Magazine*, **57**(5), pp. 73-93.
3. Sirenko, Y. and Velychko, L. (eds.), (2016) *Electromagnetic Waves in Complex Systems*, New York: Springer.
4. Sirenko, Y. and Strom, S. (eds.), (2010), *Modern Theory of Gratings. Resonant Scattering: Analysis Techniques and Phenomena*, New York: Springer.
5. Sirenko, K., Sirenko, Y., and Yashina, N., (2010) Modeling and analysis of transients in periodic gratings. I. Fully absorbing boundaries for 2-D open problems, *Journal of the Optical Society of America A*, **27**(3), pp. 532-543.
6. Kuhn, R., (1964) *Mikrowellen Antennen*, Berlin: VEB Verlag Technik.
7. Kryzhanovskiy, V. and Shestopalov, V., (1986) A millimeter wavelength phase meter with a rotating grating, *Pribory and Tekhnika Eksperimenta*, **3**, pp. 153-154, (in Russian).
8. Shestopalov, V., (1997) *Physical Foundation of the Millimeter and Sub Millimeter Waves Technique. Vol. I. Open structures*, Utrecht, Netherland & Tokyo, Japan: VSP Books Inc.
9. Shestopalov, V., Lytvynenko, L., Masalov, S., and Sologub, V., (1973) *Wave Diffraction by Gratings*, Kharkiv, Ukraine: Kharkiv State Univ. Publ., (in Russian).
10. Shestopalov, V., Kirilenko, A., Masalov, S., and Sirenko, Y., (1986) *Resonance Wave Scattering. Vol.1. Diffraction Gratings*, Kyiv, Ukraine: Naukova Dumka Publ., (in Russian).
11. Shestopalov, V. and Sirenko, Y., (1989) *Dynamic Theory of Gratings*, Kyiv, Ukraine: Naukova Dumka Publ., (in Russian).
12. Sirenko, K., Sirenko, Y., and Yashina, N., (2010) Modeling and analysis of transients in periodic gratings. II. Resonant wave scattering, *Journal of the Optical Society of America A*, **27**(3), pp. 544-552.
13. Sirenko, K., Sirenko, Y., and Yevdokymov, A., (2018) Diffraction antennas. A ridged dielectric waveguide, *Telecommunication and Radio Engineering*, **77**(10): 839-852.
14. Sautbekov, S., Sirenko, Y., and Vertiy, A., (2013) Rigorous simulation of diffraction radiation effect: electrodynamics of periodic structures places in the surface wave field of dielectric waveguides, *Telecommunications and Radio Engineering*, **72**(14), pp. 1263-1278.
15. Vertiy, A., Sautbekov, S., Sirenko, Y., and Yashina, N., (2013) The effects of diffraction radiation in finite planar and axially symmetric periodic structures, *Fizicheskie Osnovy Priborostroeniya*, **2**(4), pp. 36-52, (in Russian).
16. Burambayeva, N., Naumenko, V., Sautbekov, S., Sirenko, Y. et al., (2016) Modeling and analysis of a fast scanning diffraction radiation antenna, *Telecommunications and Radio Engineering*, **75**(3), pp. 189-199.
17. Vertiy, A., Sirenko, Y., Pavlyuchenko, A., Poyedinchuk, A. et al., (2016) Surface-to-spatial mode conversion by a convex cylindrical diffraction grating: an experimental study, *Telecommunications and Radio Engineering*, **75**(4), pp. 297-311.
18. Vertiy, A., Sirenko, Y., Sautbekov, S., Balabekov, K. et al., (2017) Formation of converging beams by diffraction radiation antennas in the millimeter wavelength range, *Telecommunications and Radio Engineering*, **76**(9), pp. 761-775.